

# Phase diagram of the $t$ - $U^2$ Hamiltonian of the weak coupling Hubbard model

Takashi Yanagisawa<sup>a,b</sup>

<sup>a</sup> Condensed-Matter Physics Group, Nanoelectronics Research Institute,

National Institute of Advanced Industrial Science and Technology (AIST) Central 2, 1-1-1 Umezono, Tsukuba 305-8568, Japan

<sup>b</sup>CREST, Japan Science and Technology Agency (JST), Kawaguchi, Saitama 332-0012, Japan

(Dated:)

We determine the symmetry of Cooper pairs, on the basis of the perturbation theory in terms of the Coulomb interaction  $U$ , for the two-dimensional Hubbard model on the square lattice. The phase diagram is investigated in detail. The Hubbard model for small  $U$  is mapped onto an effective Hamiltonian with the attractive interaction using the canonical transformation:  $H_{eff} = e^S H e^{-S}$ . The gap equation of the weak coupling formulation is solved without numerical ambiguity to determine the symmetry of Cooper pairs. The superconducting gap crucially depends on the position of the van Hove singularity. We show the phase diagram in the plane of the electron filling  $n_e$  and the next nearest-neighbor transfer  $t'$ . The  $d$ -wave pairing is dominant for the square lattice in a wide range of  $n_e$  and  $t'$ . The  $d$ -wave pairing is also stable for the square lattice with anisotropic  $t'$ . The three-band  $d$ - $p$  model is also investigated, for which the  $d$ -wave pairing is stable in a wide range of  $n_e$  and  $t_{pp}$  (the transfer between neighboring oxygen atoms). In the weak coupling analysis, the second-neighbor transfer parameter  $-t'$  could not be so large so that the optimum doping rate is in the range of  $0.8 < n_e < 0.85$ .

PACS numbers: 74.20.-z, 71.10.Fd, 75.40.Mg

## I. INTRODUCTION

Since the discovery of high-temperature superconductors, the strongly correlated electron systems have been studied intensively. The effect of the strong correlation between electrons is important for many quantum critical phenomena such as unconventional superconductivity (SC). High-temperature superconductors[1, 2, 3] as well as heavy fermions[4, 5, 6, 7] are known as the typical correlated electron systems. These systems are modeled by the Hamiltonian with the electronic interaction of the on-site Coulomb repulsion. Recently the mechanisms of superconductivity in high-temperature superconductors have been extensively studied using the two-dimensional Hubbard model[8, 9, 10, 11, 12, 13, 14, 15, 16].

The superconductivity of the Hubbard model has been questioned for many years. It is extremely difficult to show the existence of superconducting phase for the Hubbard model in a reasonable way. For the present we cannot answer this long-standing question soon. Instead of examining the possibility of superconductivity, it is possible to investigate possible symmetries of Cooper pairs for an effective Hamiltonian with the attractive interaction. For this purpose effective Hamiltonians have been obtained for the Hubbard model. The  $t$ - $J$  model is the well known effective Hamiltonian derived in the limit of the large on-site repulsion  $U$ , using the canonical transformation  $H_{t-J} = e^S H e^{-S}$  with  $S \propto t/U$ . On the other hand, in the limit of small  $U$ , the perturbation theory also leads to an effective Hamiltonian with the attractive interaction[17, 18, 19, 20], where we have  $S \propto U/t$ . The phase diagram with respect to the Cooper pair symmetry can be determined if we solve the gap equation.

We must notice that we should compare the energy with other electronic states to show that the supercon-

ducting state is indeed stable. For the half-filled band with vanishing  $t' = 0$  in two space dimensions, the antiferromagnetic order parameter for small  $U$  is[21]

$$\Delta_{AF} = \frac{8tc}{U} \exp\left(-\sqrt{\frac{4\pi^2 tc}{U}}\right), \quad (1)$$

where  $c = 3 - \sqrt{3}$ . It is, however, obvious that the antiferromagnetically ordered state is unstable away from half filling if the Coulomb repulsion  $U$  is small. Thus we focus on the case of small  $U$  for which we have also a merit that the gap equation is considerably simplified. The purpose of the paper is to determine the gap symmetry for the square lattice using the small- $U$  gap equation derived for the effective Hamiltonian. Although the real superconductivity in correlated electron systems should be described by a theory of strong-coupling superconductivity, the phase diagram can be determined in detail using the weak coupling formulation. Precise calculations are sometimes not easy at low temperatures in the strong-coupling formulation due to the Matsubara frequency summation and the wave number summation. It is important to examine the detailed phase diagram for materials belonging to strongly correlated systems such as the cuprate high temperature superconductors, the organic superconductors, the ruthenate superconductor  $\text{Sr}_2\text{RuO}_4$ .

The paper is organized as follows. In Section II the effective Hamiltonian is derived using the canonical transformation. We show that we can derive the attractive effective Hamiltonian using some approximations. In Section III the gap equation is shown and the results are presented in Section IV. We give a summary in Section V.

## II. EFFECTIVE HAMILTONIAN

The Hubbard Hamiltonian is

$$H = -t \sum_{\langle ij \rangle \sigma} (c_{i\sigma}^\dagger c_{j\sigma} + \text{h.c.}) - t' \sum_{\ll j\ell \gg \sigma} (c_{j\sigma}^\dagger c_{\ell\sigma} + \text{h.c.}) + U \sum_i n_{i\uparrow} n_{i\downarrow} \quad (2)$$

where  $\langle ij \rangle$  and  $\ll j\ell \gg$  denote the nearest-neighbor and next-nearest-neighbor pairs, respectively.  $U$  is the on-site Coulomb repulsion. The unit of energy is given by  $t$  in this paper. The total number of sites and the number of electrons are denoted as  $N$  and  $N_e$ , respectively. The half-filled band corresponds to  $n_e = N_e/N = 1$ .

The effective Hamiltonian is derived using the perturbation theory for small  $U$ . The canonical transformation also maps the Hubbard model to an effective Hamiltonian with the attractive interaction[22]. Since no instability except superconductivity occurs for small  $U$  away from half filling, we assume that the pairing interaction is the most singular. The procedure of mapping is as follows. The Hamiltonian is written as

$$H = H_0 + H_1 + H_2 + H_3, \quad (3)$$

where

$$H_0 = \sum_{k\sigma} \xi_k c_{k\sigma}^\dagger c_{k\sigma}, \quad (4)$$

$$H_1 = \frac{U}{N} \sum_{k \neq k'} c_{k'\uparrow}^\dagger c_{-k'\downarrow}^\dagger c_{-k\downarrow} c_{k\uparrow}, \quad (5)$$

$$H_2 = \frac{U}{N} \sum_{k \neq k', q \neq 0} c_{k'\uparrow}^\dagger c_{-k'-q\downarrow}^\dagger c_{-k-q\downarrow} c_{k\uparrow}, \quad (6)$$

$$H_3 = \frac{U}{N} \sum_{kk'} c_{k\uparrow}^\dagger c_{k\uparrow} c_{k'\downarrow}^\dagger c_{k'\downarrow}. \quad (7)$$

The dispersion relation  $\epsilon_k$  for the square lattice is

$$\epsilon_k = -2t(\cos k_x + \cos k_y) - 4t' \cos k_x \cos k_y, \quad (8)$$

where  $\mu$  is the chemical potential. We set  $\xi_k = \epsilon_k - \mu$ . Using a canonical transformation,  $\tilde{\psi} = e^S \psi$ , we look for the solution of the Schrödinger equation  $H_{eff} \tilde{\psi} = E \tilde{\psi}$ . The effective Hamiltonian reads

$$\begin{aligned} H_{eff} &= e^S H e^{-S} = H + [S, H] + \frac{1}{2}[S, [S, H]] + \dots \\ &= H_0 + H_1 + H_2 + H_3 + [S, H_0 + H_1 + H_2 + H_3] \\ &\quad + \frac{1}{2}[S, [S, H_0]] + \dots \end{aligned} \quad (9)$$

We determine  $S$  so as to satisfy  $H_2 + [S, H_0] = 0$ . We find

$$S = \frac{U}{N} \sum_{k \neq k', q \neq 0} \frac{1}{\xi_{k'+q} + \xi_{k'} - \xi_{k+q} - \xi_k} c_{k'\uparrow}^\dagger c_{-k'-q\downarrow}^\dagger c_{-k-q\downarrow} c_{k\uparrow}. \quad (10)$$

Since  $[S, H_3] = 0$ , we obtain up to the order of  $U^2$ ,

$$H_{eff} = H_0 + H_1 + H_3 + [S, H_1] + \frac{1}{2}[S, H_2]. \quad (11)$$

The commutator  $[S, H_2]$  is evaluated as

$$\begin{aligned} [S, H_2] &= \left(\frac{U}{N}\right)^2 \sum_{k \neq k', q \neq 0} \sum_{p \neq p', q' \neq 0} S_{kk'}^q \\ &\quad \times (-\delta_{pk'} c_{p'\uparrow}^\dagger c_{-p'-q'\downarrow}^\dagger c_{-p-q'\downarrow} c_{-k'-q\downarrow} c_{-k-q\downarrow} c_{k\uparrow} \\ &\quad + \delta_{p+q', k'+q} c_{p'\uparrow}^\dagger c_{-p'-q'\downarrow}^\dagger c_{k'\uparrow}^\dagger c_{p\uparrow} c_{-k-q\downarrow} c_{k\uparrow} \\ &\quad - \delta_{p'+q', k+q} c_{k'\uparrow}^\dagger c_{-k'-q\downarrow}^\dagger c_{p'\uparrow}^\dagger c_{k\uparrow} c_{-p-q'\downarrow} c_{p\uparrow} \\ &\quad + \delta_{p'k} c_{k'\uparrow}^\dagger c_{-k'-q\downarrow}^\dagger c_{-k-q\downarrow} c_{-p'-q'\downarrow} c_{-p-q'\downarrow} c_{p\uparrow}), \end{aligned} \quad (12)$$

where

$$S_{kk'}^q = \frac{1}{\xi_{k'+q} + \xi_{k'} - \xi_{k+q} - \xi_k}. \quad (13)$$

Since the purpose of this paper is to investigate the pairing symmetry, we need only the first term and the last term of  $[S, H_2]$ . We find that the average of the second and third terms with respect to the BCS wave function vanish. Due to the same reason  $[S, H_1]$  can be neglected. Then the effective Hamiltonian is

$$\begin{aligned} H_{t-U^2} &= \sum_{k\sigma} \xi_k c_{k\sigma}^\dagger c_{k\sigma} + \frac{U}{N} \sum_{k \neq k'} c_{k'\uparrow}^\dagger c_{-k'\downarrow}^\dagger c_{-k\downarrow} c_{k\uparrow} \\ &\quad + \frac{1}{2} \frac{U^2}{N^2} \sum_{k \neq k', q \neq 0} \sum_{p \neq p', q' \neq 0} \frac{1}{\xi_{k'+q} + \xi_{k'} - \xi_{k+q} - \xi_k} \\ &\quad \cdot (\delta_{p'k} c_{k'\uparrow}^\dagger c_{-k-q\downarrow}^\dagger c_{-k'-q\downarrow}^\dagger c_{-p-q'\downarrow} c_{-p'-q'\downarrow} c_{p\uparrow} \\ &\quad - \delta_{pk'} c_{p'\uparrow}^\dagger c_{-p-q'\downarrow}^\dagger c_{-p'-q'\downarrow}^\dagger c_{-k-q\downarrow} c_{-k'-q\downarrow} c_{k\uparrow}), \end{aligned} \quad (14)$$

If we set  $k = p + q'$  and  $p' = k' + q$ , the first term of

$[S, H_2]$  is approximated as

$$\begin{aligned}
H_{2a} &\equiv -\left(\frac{U}{N}\right)^2 \sum_{k \neq k', q \neq 0} \sum_{p \neq p', q' \neq 0} S_{k'k}^q \delta_{pk'} \\
&\times c_{p'\uparrow}^\dagger c_{-p'-q'\downarrow}^\dagger c_{-p-q'\downarrow} c_{-k'-q\downarrow}^\dagger c_{-k-q\downarrow} c_{k\uparrow} \\
&\approx \left(\frac{U}{N}\right)^2 \sum_{k \neq k', q \neq 0} c_{k'+q\uparrow}^\dagger c_{-k'-q\downarrow}^\dagger \frac{c_{-k-q\downarrow}^\dagger c_{-k-q\downarrow}}{\xi_{k'+q} + \xi_{k'} - \xi_{k+q} - \xi_k} \\
&\times c_{-k\downarrow} c_{k\uparrow} \\
&\approx \left(\frac{U}{N}\right)^2 \sum_{k \neq k'-q, q \neq 0} c_{k'\uparrow}^\dagger c_{-k'\downarrow}^\dagger \frac{f_{-k-q}}{\xi_{k'} + \xi_{k'-q} - \xi_{k+q} - \xi_k} \\
&\times c_{-k\downarrow} c_{k\uparrow} \\
&= \left(\frac{U}{N}\right)^2 \sum_{k+q \neq 0, k'+q \neq 0} c_{k'\uparrow}^\dagger c_{-k'\downarrow}^\dagger \\
&\times \frac{f_q}{\xi_{k'+k+q} - \xi_{-q} + \xi_{k'} - \xi_k} c_{-k\downarrow} c_{k\uparrow}
\end{aligned} \tag{15}$$

where  $f_k$  is the Fermi distribution function,

$$f_k = \frac{1}{e^{\beta \xi_k} + 1}. \tag{16}$$

Since the summation is restricted to the small region near the Fermi surface, we obtain assuming  $\xi_{-k} = \xi_k$

$$H_{2a} \approx \left(\frac{U}{N}\right)^2 \sum_{k \neq -q, k' \neq -q} \frac{f_q}{\xi_{k'+k+q} - \xi_q} c_{k'\uparrow}^\dagger c_{-k'\downarrow}^\dagger c_{-k\downarrow} c_{k\uparrow}. \tag{17}$$

Similarly the last term of  $[S, H_2]$  is written as

$$H_{2b} \approx \left(\frac{U}{N}\right)^2 \sum_{k \neq -q, k' \neq -q} \frac{f_{k'+k+q}}{\xi_{k'+k+q} - \xi_q} c_{k'\uparrow}^\dagger c_{-k'\downarrow}^\dagger c_{-k\downarrow} c_{k\uparrow}. \tag{18}$$

The resulting effective Hamiltonian is

$$\begin{aligned}
H_{eff} &= e^S H e^{-S} \equiv H_{t-U^2} \\
&= \sum_{k\sigma} \xi_k c_{k\sigma}^\dagger c_{k\sigma} + \sum_{kk'} V_{kk'} c_{k'\uparrow}^\dagger c_{-k'\downarrow}^\dagger c_{-k\downarrow} c_{k\uparrow},
\end{aligned} \tag{19}$$

where

$$V_{kk'} = \frac{U}{N} + \frac{U^2}{N} \chi(\mathbf{k} + \mathbf{k}'). \tag{20}$$

$\chi(k + k')$  is the magnetic susceptibility defined as

$$\chi(\mathbf{k} + \mathbf{k}') = \frac{1}{N} \sum_q \frac{f_{k+k'+q} - f_q}{\xi_q - \xi_{k+k'+q}}. \tag{21}$$

Thus we have reached the effective Hamiltonian up to the order of  $U^2$  using the canonical transformation.

### III. GAP EQUATION

The gap equation for the  $t-U^2$  model was investigated in Ref.[19]. Since the equation was considerably simplified for small  $U$ , the gap equation was solved without numerical ambiguity. We define the order parameter,

$$\Delta_k = \sum_{k'} V_{kk'} \langle c_{-k'\downarrow} c_{k'\uparrow} \rangle. \tag{22}$$

Using the mean-field theory, the gap equation for the Hamiltonian  $H_{t-U^2}$  is

$$\Delta_k = - \sum_{k'} V_{kk'} \Delta_{k'} \frac{1 - 2f(E_{k'})}{2E_{k'}}, \tag{23}$$

where  $E_k = \sqrt{\xi_k^2 + \Delta_k^2}$ . We assume the anisotropic order parameter given as

$$\Delta_{\mathbf{k}} = \Delta \cdot z_{\mathbf{k}}, \tag{24}$$

where  $z_{\mathbf{k}}$  denotes the  $\mathbf{k}$ -dependence of  $\Delta_{\mathbf{k}}$ . At  $T = 0$  the gap equation is written as

$$\Delta_k = -\frac{1}{2} \sum_{k'} V_{kk'} \frac{\Delta_{k'}}{E_{k'}}. \tag{25}$$

For small  $U$ , the gap equation for anisotropic pairing is extremely simplified retaining only the logarithmic term[19]:

$$z_{\mathbf{k}} = \log\left(\frac{\Delta}{2\omega_0}\right) U^2 \frac{1}{N} \sum_{k'} \chi(\mathbf{k} + \mathbf{k}') \delta(\xi_{k'}) z_{k'}, \tag{26}$$

where  $\omega_0$  is the cut-off energy. The critical temperature  $T_c$  is determined by

$$z_{\mathbf{k}} = - \sum_{k'} V_{\mathbf{k}\mathbf{k}'} z_{\mathbf{k}'} \frac{1 - 2f(|\xi_{k'}|)}{2|\xi_{k'}|}, \tag{27}$$

for  $T = T_c$ . For small  $U$ , the critical temperature  $T_c$  is extremely small. In this case we can use the following approximation,

$$\begin{aligned}
I &\equiv \int_0^{\omega_0} d\xi g(\xi) \frac{\tanh(\beta_c \xi/2)}{\xi} \\
&\approx g(\omega_0) \log \omega_0 - \frac{\beta_c}{2} \int_0^{\omega_0} d\xi \log \xi \cdot g(\xi) \frac{1}{(\cosh(\beta_c \xi/2))^2} \\
&= g(\omega_0) \log \omega_0 - \int_0^{\beta_c \omega_0/2} dx \log\left(\frac{2x}{\beta_c}\right) g\left(\frac{2x}{\beta_c}\right) \frac{1}{(\cosh x)^2} \\
&= g(\omega_0) \log \omega_0 - g(0) \int_0^{\beta_c \omega_0/2} dx \log\left(\frac{2x}{\beta_c}\right) \frac{1}{(\cosh x)^2} \\
&\approx g(0) \log\left(\frac{2e^\gamma \omega_0}{\pi k_B T_c}\right),
\end{aligned} \tag{28}$$

where we assume that  $g(\xi)$  is a slowly varying function and  $g'(\xi)$  is negligible. The equation is written as

$$z_{\mathbf{k}} = -\log\left(\frac{2e^\gamma \hbar \omega_0}{\pi k_B T_c}\right) \sum_{k'} V_{\mathbf{k}\mathbf{k}'} z_{\mathbf{k}'} \delta(\xi_{k'}). \tag{29}$$

Since  $T_c$  is very small, the summation over  $\mathbf{k}'$  can be restricted to the average over near the Fermi surface. If we solve the eigenequation

$$\frac{2}{N} \sum_{\mathbf{k}'} \chi(\mathbf{k} + \mathbf{k}') z_{\mathbf{k}'} \delta(\xi_{\mathbf{k}'}) = -x z_{\mathbf{k}}, \quad (30)$$

the critical temperature is obtained as

$$k_B T_c = 1.13 \omega_0 \exp\left(-\frac{2t^2}{xU^2}\right), \quad (31)$$

where the energy unit is given by  $t$ . Since  $\Delta$  is given as

$$\Delta = 2\omega_0 \exp\left(-\frac{2t^2}{xU^2}\right), \quad (32)$$

the ratio  $2\Delta/k_B T_c$  equals the BCS universal value  $2\pi/e^\gamma = 3.53$ .

#### IV. PAIRING SYMMETRY

##### A. Method of solving the eigenvalue equation

We express  $z_{\mathbf{k}}$  and  $V_{\mathbf{k}\mathbf{k}'}$  in terms of the polar coordinates[19]:

$$z_{\mathbf{k}} = z(\xi, \theta), \quad (33)$$

$$\chi(\mathbf{k} + \mathbf{k}') = \chi(\xi, \theta, \xi', \theta'), \quad (34)$$

where  $\mathbf{k}$  is expressed using the polar angle  $\theta$ :  $\mathbf{k} = (\xi, \theta)$  in terms of the polar coordinates. We consider the gap function on the Fermi surface  $z(\theta) \equiv z(0, \theta)$ . If we define  $\chi(\theta, \theta') = \chi(0, \theta, 0, \theta')$ , the gap equation is

$$2 \int_0^{2\pi} d\theta' \rho_F(\theta') \chi(\theta, \theta') z(\theta') = -x z(\theta), \quad (35)$$

where  $\rho_F(\theta)$  is the density of states at the Fermi surface:

$$\rho_F(\theta) = \frac{1}{(2\pi)^2} k_F(\theta) \frac{1}{\left| \frac{\partial \xi}{\partial k}(k = k_F(\theta)) \right|}, \quad (36)$$

where  $k_F(\theta)$  is the Fermi wave number of the polar coordinate  $\theta$  and  $\partial \xi / \partial k$  is the derivative with respect to  $k = |\mathbf{k}|$ . If we expand  $z(\theta)$  as

$$z(\theta) = \sum_n z_n e^{in\theta}, \quad (37)$$

the gap equation is given as

$$\sum_n \chi_{mn} z_n = -x z_m, \quad (38)$$

where  $\chi_{mn}$  are the matrix elements of  $\chi(\theta, \theta')$ :

$$\chi_{mn} = \frac{1}{\pi} \int_0^{2\pi} d\theta d\theta' \rho_F(\theta') e^{-im\theta} \chi(\theta, \theta') e^{in\theta'}. \quad (39)$$

The number of basis functions kept in solving the eigenequation is 30 to 40 in this paper. The  $\mathbf{k}$ -space is divided into  $200 \times 200$  points on an equally spaced mesh in the numerical calculations of  $\chi(\theta, \theta')$ .

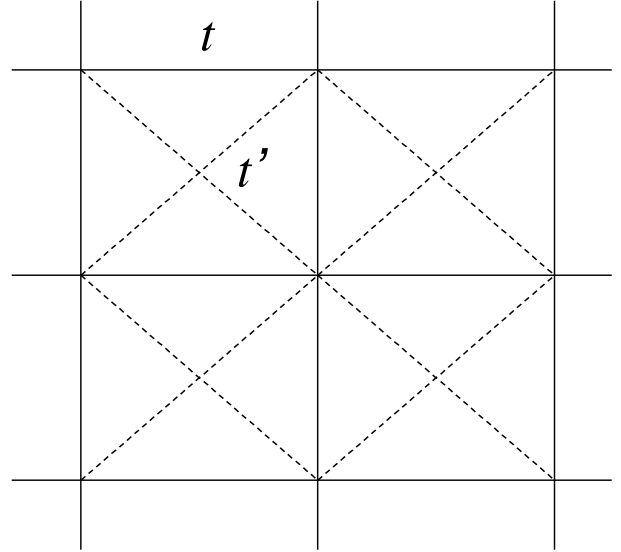


FIG. 1: Square lattice with next-nearest transfer  $t'$ .

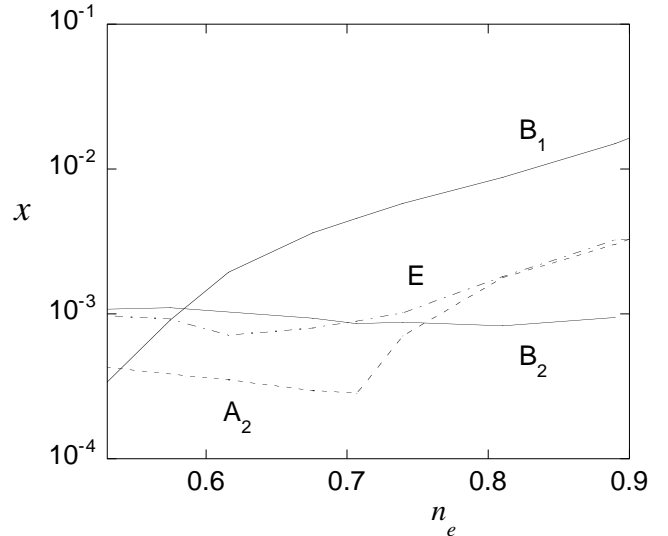


FIG. 2: The exponent  $x$  as a function of the electron density for  $t' = 0$ . (See [19]. We have included  $x$  for the E representation.) Since the line for  $A_1$  mostly coincides with that for  $B_2$ , the  $A_1$  line is omitted.

##### B. Simple square lattice

Let us investigate the phase diagram for the square lattice (Fig.IV A). The basis functions  $\{e^{in\theta}\}$  ( $n = 0, \pm 1, \pm 2, \dots$ ) are classified into irreducible representations according to the symmetry group. The eigenfunctions are specified by one of irreducible representations

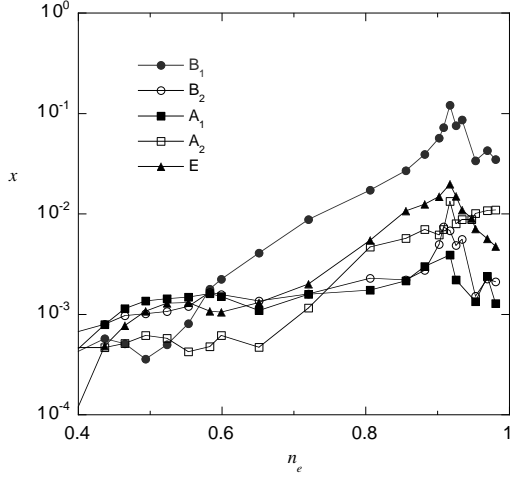


FIG. 3: The exponent  $x$  as a function of the electron density for  $t' = -0.1$ .

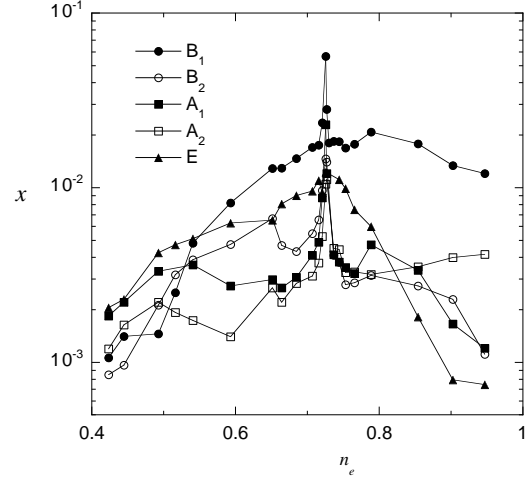


FIG. 5: The exponent  $x$  as a function of the electron density for  $t' = -0.3$ .

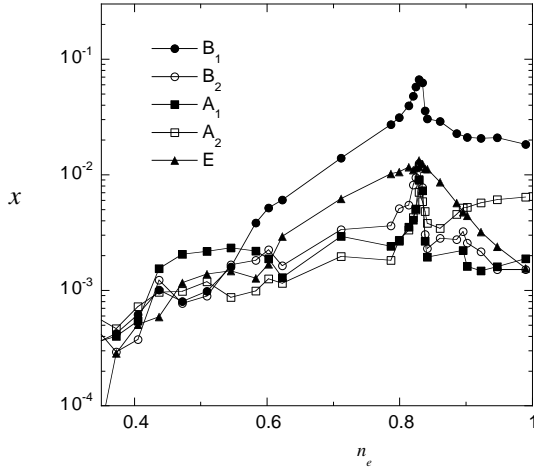


FIG. 4: The exponent  $x$  as a function of the electron density for  $t' = -0.2$ .

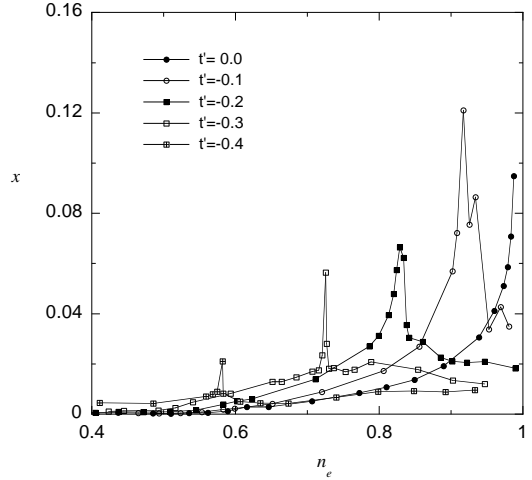


FIG. 6: The exponent  $x$  of  $B_1$  symmetry as a function of the electron density for  $t' = 0, -0.1, -0.2, -0.3$  and  $-0.4$ .

of the square lattice (see Table 1). It is convenient to use real basis functions  $\cos(n\theta)$  and  $\sin(n\theta)$  for this purpose. The gap function in each representation is[19]

$$z(\theta) = \sum_{\ell=1} z_{4\ell} \cos(4\ell\theta) \quad A_1, \quad (40)$$

$$z(\theta) = \sum_{\ell=1} z_{4\ell} \sin(4\ell\theta) \quad A_2, \quad (41)$$

$$z(\theta) = \sum_{\ell=1} z_{4\ell-2} \cos(4\ell-2)\theta \quad B_1, \quad (42)$$

$$z(\theta) = \sum_{\ell=1} z_{4\ell-2} \sin(4\ell-2)\theta \quad B_2. \quad (43)$$

$$z(\theta) = \sum_{\ell=1} z_{2\ell-1} \cos(2\ell-1)\theta \quad \text{or} \quad \sin(2\ell-1)\theta \quad E. \quad (44)$$

In Ref.[19] the representations  $A_1 \sim B_2$  were investigated. Here the E symmetry for triplet pairing is also examined. The eigenequation is solved for the above shown basis functions in the space of each irreducible representation. The eigenvalue  $x$  for  $t' = 0$  is shown in Fig.IV A as a function of the electron density  $n_e$ . For  $n_e > 0.6$  the

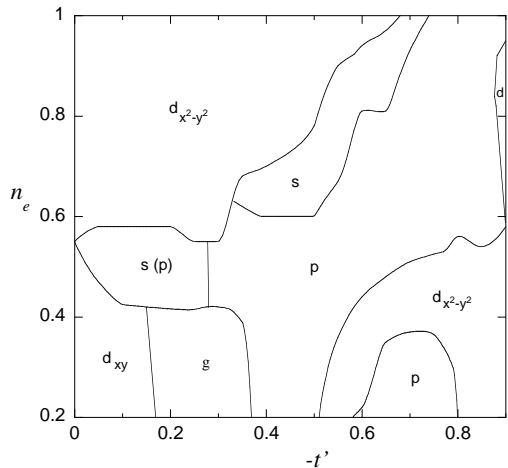


FIG. 7: Phase diagram in the  $n_e-t'$  plane for  $t' \leq 0$ .  $s$  denotes the pairing state with extended- $s$  wave symmetry. In the  $s$ -wave region for small  $|t'|$ , the  $s$ - and  $p$ -wave states are sometimes nearly degenerate. Small regions near boundaries are not shown.

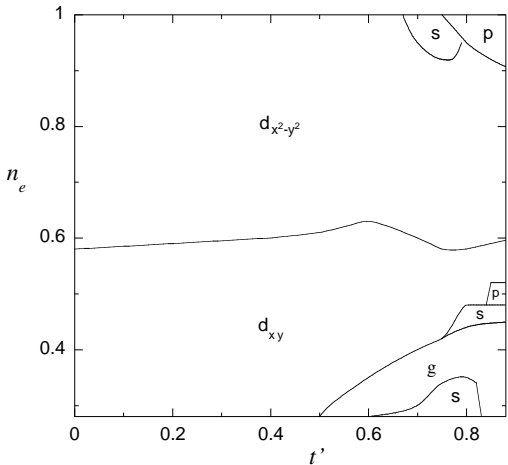


FIG. 8: Phase diagram in the  $n_e-t'$  plane for  $t' \geq 0$ .  $s$ ,  $g$  and  $d_{x^2-y^2}$  wave pairing states are almost degenerate in the low-carrier region for large  $t'$ .

paired state with  $d_{x^2-y^2}$  symmetry is most stable for  $t' = 0$ . Since the exponent  $x$  sensitively depends on the van Hove singularity,  $x$  is an increasing function of  $n_e$  near half filling for  $t' = 0$ .

The exponent  $x$  for  $t' = -0.1$ ,  $-0.2$  and  $-0.3$  is shown in Figs. IV A, IV A and IV A, respectively. The exponents for small electron filling are not shown here because the high numerical accuracy is required for exponentially small exponents. As is shown in the figures, the  $d$ -wave state is most stable near half-filled case for  $t'$  in the range

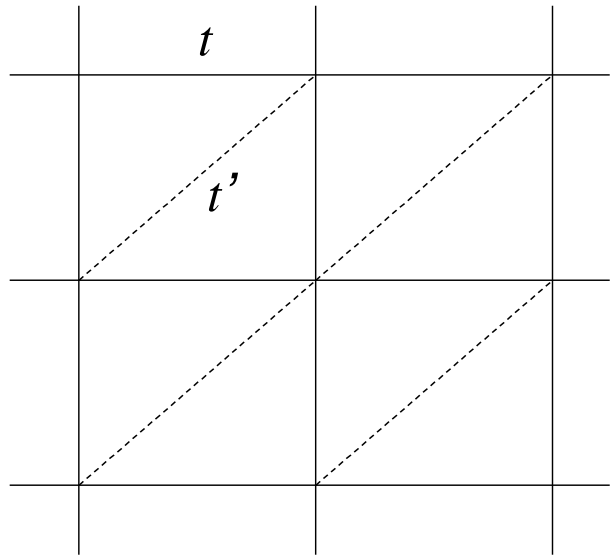


FIG. 9: Square lattice with anisotropic next-nearest transfer  $t'$  (anisotropic triangular lattice) which is the lattice of organic conductors.

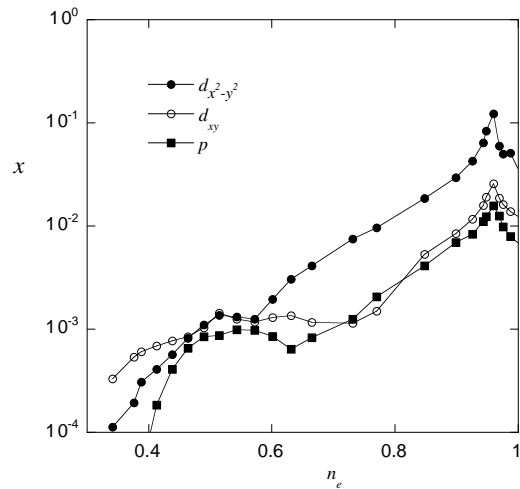


FIG. 10: The exponent  $x$  on the square lattice with anisotropic  $t' = -0.1$ .

of  $0 \leq t' \leq 0.4$ . The position of the van Hove singularity depends on  $t'$ , and the peak of  $x$  shifts as  $-t' > 0$  increases (Fig. IV A).  $x$  has a sharp peak showing a logarithmic increase due to the van Hove singularity:

$$x \sim -\log|\mu - \mu_{vH}|, \quad (45)$$

where  $\mu_{vH}$  is the chemical potential corresponding to

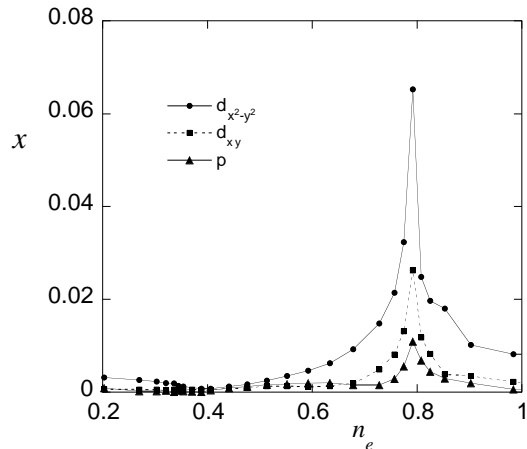


FIG. 11: The exponent  $x$  on the square lattice with anisotropic  $t' = -0.5$ .

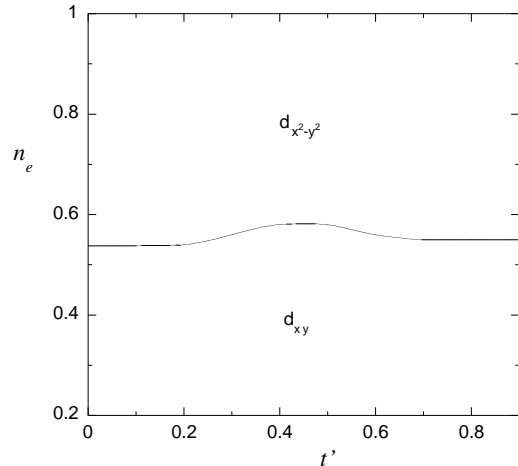


FIG. 13: Phase diagram for the square lattice with anisotropic  $t' > 0$  (lattice of organic conductors).

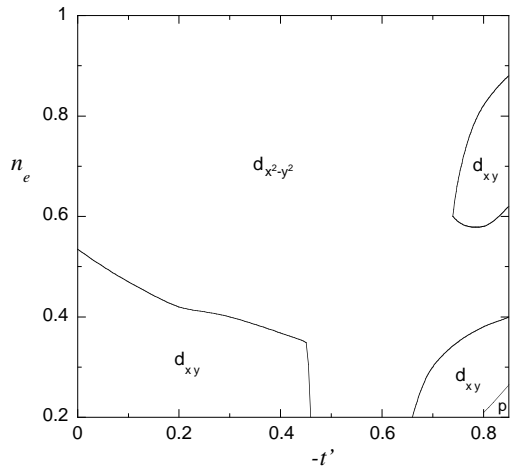


FIG. 12: Phase diagram for the square lattice with anisotropic  $t' < 0$  (lattice of organic conductors).

the van Hove singularity. The figure suggests higher  $T_c$  for small  $-t'$ . The antiferromagnetism, however, may compete and suppress superconductivity near half filling. Hence we must have a bell-shape critical temperature as a function of the electron filling.

It was pointed out from the electronic states calculations that the Fermi surface is much deformed for  $\text{Tl}_2\text{Ba}_2\text{CuO}_6$ , [23] and  $\text{HgBa}_2\text{CuO}_4$  [24] for which the band parameter values must be assigned as  $t' \sim -0.4$  and  $t'' \sim 0.1$  (third-neighbor transfer).  $\text{Bi}_2\text{Sr}_2\text{CaCu}_2\text{O}_{8+\delta}$  (Bi2212) also has deformed Fermi surface so that  $t' \sim -0.3$  and  $t'' \sim 0.2$  [25]. For these values the optimum doping rate must be larger than that for  $\text{La}_{1-x}\text{Sr}_x\text{CuO}_4$  (LSCO) for which  $t' \sim -0.1$  and  $t'' \sim 0$ . Experiments,

however, indicated that the optimum doping rate is almost the same for Bi2212 and LSCO [26]. This may be a flaw of the weak coupling formulation, which, however, may not be completely remedied by the strong coupling treatment since the van Hove singularity still has a large effect on the critical temperature. This suggests that we must reexamine the structure of the Fermi surface of high temperature cuprates. In particular, the band parameters for Bi2212 will be modified if we take into account the double layer structure [27, 28]. The band structure reported by recent studies [28, 29] is well fitted using smaller  $t'$  such as [30]

$$t' \sim -0.2. \quad (46)$$

The phase diagram in the  $n_e$ - $t'$  plane is shown in Fig. IV A for  $t' \leq 0$  and in Fig. IV A for  $t' \geq 0$ . For  $n_e \sim 0.5$  and  $-t' \sim 0.4$ , there is a possibility that the  $p$ -wave superconductivity is realized. For example, the ruthenate superconducting material  $\text{Sr}_2\text{RuO}_4$  [31] is sometimes modeled by the one-band Hubbard model for the  $\gamma$  orbital with  $t' \sim -0.4$  and  $n_e \simeq 0.67$  after the electron-hole transformation. The state of these parameters just corresponds to the point within the singlet region near the boundary to  $p$ -wave regions in Fig. IV A. In order to obtain the stable  $p$ -wave pairing for the parameters corresponding to  $\text{Sr}_2\text{RuO}_4$ , we may need to consider the multi-band structure including  $\alpha$  and  $\beta$  orbitals [32]. For  $t' > 0$  we have a large  $d$ -wave region.

If  $t'$  is large and negative, i.e. if  $-t' > 0.5$ , we have the case with two Fermi surfaces; one is a large Fermi surface (FS1) and the other is a small Fermi surface (FS2) inside of the larger one. In this case we must examine the coupled equation of two gap functions  $z_k^1$  and  $z_k^2$  cor-

TABLE I: Irreducible representations of  $C_{4v}$  for the square lattice. One of basis functions are also shown.

Rep.	Symmetry	Bases		
$A_1$	$s$	1		$\cos(4\theta)$
$A_2$	$g$	$xy(x^2 - y^2)$		$\sin(4\theta)$
$B_1$	$d_{x^2-y^2}$	$\cos(k_x) - \cos(k_y)$	$x^2 - y^2$	$\cos(2\theta)$
$B_2$	$d_{xy}$	$\sin(k_x)\sin(k_y)$	$xy$	$\sin(2\theta)$
$E$	$p$	$\sin(k_x), \sin(k_y)$	$x, y$	$\cos(\theta), \sin(\theta)$

responding to two Fermi surfaces:

$$\frac{2}{N} \sum_{\mathbf{k}':FS1} \chi^{11}(\mathbf{k}+\mathbf{k}') z_{\mathbf{k}'}^1 \delta(\xi_{\mathbf{k}'}) + \frac{2}{N} \sum_{\mathbf{k}':FS2} \chi^{12}(\mathbf{k}+\mathbf{k}') z_{\mathbf{k}'}^2 = -x z_{\mathbf{k}}^1 \quad (47)$$

$$\frac{2}{N} \sum_{\mathbf{k}':FS1} \chi^{21}(\mathbf{k}+\mathbf{k}') z_{\mathbf{k}'}^1 \delta(\xi_{\mathbf{k}'}) + \frac{2}{N} \sum_{\mathbf{k}':FS2} \chi^{22}(\mathbf{k}+\mathbf{k}') z_{\mathbf{k}'}^2 = -x z_{\mathbf{k}}^2 \quad (48)$$

where the symbol  $\sum_{\mathbf{k}':FSi}$  indicates the summation over the Fermi surface  $FSi$  and  $\chi^{ij}(\mathbf{k}+\mathbf{k}')$  is the susceptibility for  $\mathbf{k}$  on  $FSi$  and  $\mathbf{k}'$  on  $FSj$ . The stable pairing symmetry is also obtained using the electron-hole transformation for  $t' > 0$  for which we have almost only one Fermi surface even in the electron-doped case.

### C. Square lattice with anisotropic $t'$

The Hubbard model on the square lattice with anisotropic next-nearest-neighbor transfer  $t'$  (Fig.IV A) has been investigated intensively as a model for organic conductors such as BDET-TTF(ET) molecules[33, 34, 35] The model for organic conductors is well known as the Hubbard model with anisotropic next-nearest neighbor transfer  $t'$  (which is sometimes called the anisotropic triangular lattice). The dispersion relation is

$$\xi_k = -2t(\cos k_x + \cos k_y) - 2t' \cos(k_x + k_y) - \mu, \quad (49)$$

This model has the two-fold rotational symmetry and we classify the irreducible representation using the  $C_{2v}$  point group (Table 2). The exponent  $x$  is in Figs.IV A and IV A as a function of the electron density  $n_e$  for  $t' = -0.1$  and  $t' = -0.5$ , respectively. As apparent from the figures, the  $d$ -wave state is stable over the whole region, which is consistent with the FLEX prediction[36]. The phase diagram in the  $n_e$ - $t'$  plane is presented in Fig.IV A for  $t' < 0$  and in Fig.IV A for  $t' > 0$ . For this model we conclude that the  $d$ -wave pairing is stable over the whole range of parameters.

### D. Three-band $d$ - $p$ model

The formulation is also applied to the three-band model for the  $\text{CuO}_2$  plane[37]. We are interested in

TABLE II: Irreducible representations of  $C_{2v}$  for the square lattice with anisotropic next-nearest-neighbor transfer.

Representation	Symmetry	Bases	
$A_1$	$d_{x^2-y^2}$	$x^2, y^2$	$\cos(2\theta)$
$A_2$	$d_{xy}$	$xy$	$\sin(2\theta)$
$B_1$	$p_x$	$x$	$\cos(\theta)$
$B_2$	$p_y$	$y$	$\sin(\theta)$

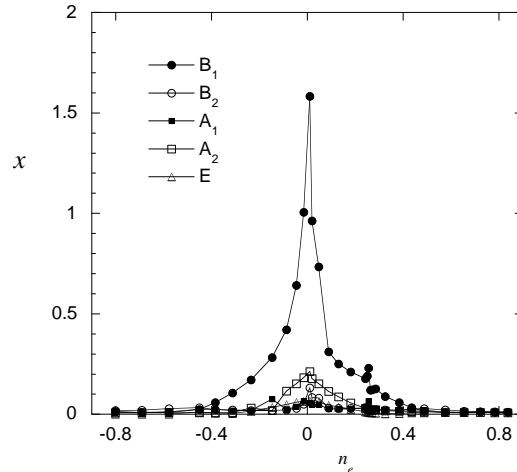


FIG. 14:  $x$  as a function of the carrier density  $n_e$  for the square lattice  $d$ - $p$  model:  $n_e > 0$  for hole doping and  $n_e < 0$  for electron doping.

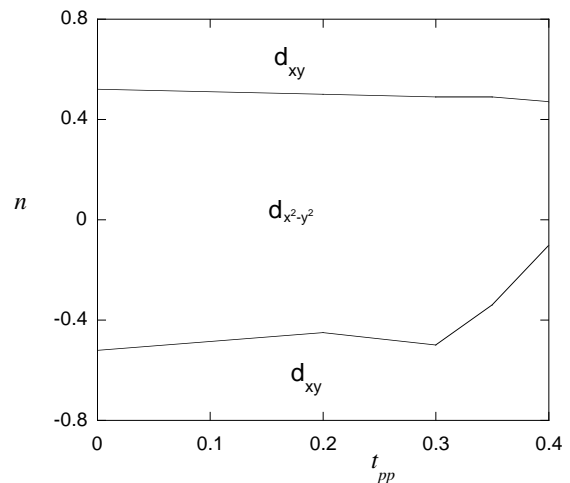


FIG. 15: Phase diagram for the three-band  $d$ - $p$  model in the plane of the carrier number  $n$  and  $t_{pp}$  in the range of  $0 \leq t_{pp} \leq 0.4$ . We set  $\epsilon_p - \epsilon_d = 2$  and  $t_{dp} = 1$ .  $n = 0$  indicates the half filling, and the positive and negative  $n$  are for hole doping and electron doping, respectively.

the relation between the single-band Hubbard model and the three-band  $d$ - $p$  model. The pairing symmetry in the electron-doped cuprates is still controversial between the  $d$ -wave and  $s$ -wave order parameter[38, 39, 40]. The Hamiltonian is

$$\begin{aligned}
H_{dp} = & \epsilon_d \sum_{i\sigma} d_{i\sigma}^\dagger d_{i\sigma} + \epsilon_p \sum_{i\sigma} (p_{i+\hat{x}/2\sigma}^\dagger p_{i+\hat{x}/2\sigma} \\
& + p_{i+\hat{y}/2\sigma}^\dagger p_{i+\hat{y}/2\sigma}) \\
& + t_{dp} \sum_{i\sigma} [d_{i\sigma}^\dagger (p_{i+\hat{x}/2\sigma} + p_{i+\hat{y}/2\sigma} - p_{i-\hat{x}/2\sigma} - p_{i-\hat{y}/2\sigma} \\
& + \text{h.c.}) + t_{pp} \sum_{i\sigma} [p_{i+\hat{y}/2\sigma}^\dagger p_{i+\hat{x}/2\sigma} - p_{i+\hat{y}/2\sigma}^\dagger p_{i-\hat{x}/2\sigma} \\
& - p_{i-\hat{y}/2\sigma}^\dagger p_{i+\hat{x}/2\sigma} + p_{i-\hat{y}/2\sigma}^\dagger p_{i-\hat{x}/2\sigma} + \text{h.c.}] \\
& + U_d \sum_i d_{i\uparrow}^\dagger d_{i\uparrow} d_{i\downarrow}^\dagger d_{i\downarrow}. \tag{50}
\end{aligned}$$

In this subsection the energy is measured in units of  $t_{dp}$ . The energy levels of the non-interacting Hamiltonian is written as in a concise form[37]:

$$\epsilon_{\mathbf{k}}^\alpha = \frac{2}{\sqrt{3}} t_{\mathbf{k}} \cos\left(\frac{\phi_{\mathbf{k}} + 2\pi\alpha}{3}\right) + \frac{\epsilon_d - \epsilon_p}{3}. \tag{51}$$

for  $\alpha = 0, 1$  and  $2$ , where

$$t_{\mathbf{k}} = \sqrt{|\eta_{\mathbf{k}}^x|^2 + |\eta_{\mathbf{k}}^y|^2 + (\eta_{\mathbf{k}}^p)^2 + (\epsilon_d - \epsilon_p)^2/3}, \tag{52}$$

$$\phi_{\mathbf{k}} = \frac{\pi}{2} + \text{sign}(s_{\mathbf{k}}) \left( \frac{\pi}{2} - \arctan \sqrt{|1 - 4t_{\mathbf{k}}^6/(27s_{\mathbf{k}}^2)|} \right), \tag{53}$$

$$s_{\mathbf{k}} = (\epsilon_d - \epsilon_p) \left( \frac{(\epsilon_d - \epsilon_p)^2}{27} - \frac{t_{\mathbf{k}}^2}{3} + (\eta_{\mathbf{k}}^p)^2 \right) + \eta_{\mathbf{k}}^p (\eta_{\mathbf{k}}^x \eta_{\mathbf{k}}^{y*} + \eta_{\mathbf{k}}^{x*} \eta_{\mathbf{k}}^y), \tag{54}$$

where  $\eta_{\mathbf{k}}^x = 2it_{dp}\sin(k_x/2)$ ,  $\eta_{\mathbf{k}}^y = 2it_{dp}\sin(k_y/2)$ , and  $\eta_{\mathbf{k}}^p = -4t_{pp}\sin(k_x/2)\sin(k_y/2)$ .  $\epsilon_{\mathbf{k}}^\alpha$  for  $\alpha = 0, 1, 2$  is the dispersion relation of the upper, lower and middle band, respectively. We examine the doped case within the hole picture where the lowest band is occupied up to the Fermi energy  $\mu$ . The effective interaction is

$$V_{\mathbf{k}\mathbf{k}'} = \frac{U_d}{N} + \frac{U_d^2}{N} \chi^{dd}(\mathbf{k} + \mathbf{k}'), \tag{55}$$

where

$$\chi^{dd}(\mathbf{q}) = \frac{1}{N} \sum_{\mathbf{p}} \sum_{\alpha\beta} w_{\mathbf{q}+\mathbf{p}}^\alpha \frac{f_{\mathbf{q}+\mathbf{p}}^\alpha - f_{\mathbf{p}}^\beta}{\epsilon_{\mathbf{p}}^\beta - \epsilon_{\mathbf{q}+\mathbf{p}}^\alpha} w_{\mathbf{p}}^\beta. \tag{56}$$

Here  $f_{\mathbf{k}}^\alpha$  is the Fermi distribution function,

$$f_{\mathbf{k}}^\alpha = \left( e^{\beta(\epsilon_{\mathbf{k}}^\alpha - \mu)} + 1 \right)^{-1}. \tag{57}$$

The weighting factor of  $d$  electrons  $w_{\mathbf{k}}^\alpha$  is defined as

$$w_{\mathbf{k}}^\alpha = \frac{(\eta_{\mathbf{k}}^p - \epsilon_{\mathbf{k}}^\alpha)(\eta_{\mathbf{k}}^p + \epsilon_{\mathbf{k}}^\alpha)}{(\epsilon_{\mathbf{k}}^\beta - \epsilon_{\mathbf{k}}^\alpha)(\epsilon_{\mathbf{k}}^\alpha - \epsilon_{\mathbf{k}}^\gamma)}, \tag{58}$$

where  $\alpha, \beta$  and  $\gamma$  are different from each other. The gap equation is

$$\Delta_{\mathbf{k}} = - \sum_{\mathbf{k}'} w_{\mathbf{k}} V_{\mathbf{k}\mathbf{k}'}^{dd} w_{\mathbf{k}'} \Delta_{\mathbf{k}'}, \tag{59}$$

where  $w_{\mathbf{k}} = w_{\mathbf{k}}^1$  and  $E_{\mathbf{k}} = \sqrt{\xi_{\mathbf{k}}^2 + \Delta_{\mathbf{k}}^2}$  for the lowest-band dispersion  $\xi_{\mathbf{k}} = \epsilon_{\mathbf{k}}^1 - \mu$ .

$d$ -wave pairing is predominant over the whole range in the parameter space as is shown in Fig.IV C. In particular,  $d_{x^2-y^2}$ -wave pairing is stable near half-filling. Although the extended  $s$ -wave pairing is possible in the narrow region near half filling in the Gutzwiller variational Monte Carlo study[14], we have no chance of  $s$ -wave superconductivity within the weak-coupling perturbation theory. The phase diagram for the  $d$ - $p$  model is shown in Fig.IV C.

## V. SUMMARY

We have examined the phase diagram with respect to pairing symmetry on the basis of the two-dimensional Hubbard model. The weak coupling formulation is convenient to investigate the phase diagram in detail. The results are almost consistent with the strong-coupling perturbation theory. We summarize the results as follows.

(1) The  $d$ -wave pairing is stable near half filling for the square lattice and the anisotropic square lattice.

(2) The gap function has a maximum at the van Hove singularity. As the second neighbor transfer  $t'$  increases, the energy of the van Hove singularity decreases. For large  $t' = -0.3 \sim -0.4$ , the optimal doping is more than 25 percent doping, i.e.  $n_e < 0.75$ . For small third neighbor transfer  $t''$  the situation remains the same. The large  $-t'$  is assigned to several high-temperature cuprates to fit the angle resolved photoemission spectroscopy (ARPES) data or the Fermi surface obtained by the band structure calculations. Most of them, however, have optimum critical temperature in the range of  $0.8 < n_e < 0.85$ . Thus the weak coupling analysis suggests that we must consider other electronic or lattice interactions, or reexamine the band parameters  $t'$  and  $t''$ . Recent ARPES studies have reported the band structure which is well fitted using rather smaller  $t'$  such as  $t' \sim -0.2$  by our analysis.

(3) The predictions of the weak-coupling theory are almost consistent with the variational Monte Carlo method. An effective interaction to induce superconductivity is possibly the simple  $\chi(\mathbf{q})$  with renormalization in the Gutzwiller variational theory.

(4) For the  $d$ - $p$  model, the  $d$ -wave pairing is predominant in the wide range and the phase diagram is almost symmetric between electron and hole dopings. Although the pairing symmetry in the electron-doped cuprates is controversial, only the  $d$ -wave pairing is possible near half-filling in the weak-coupling formulation.

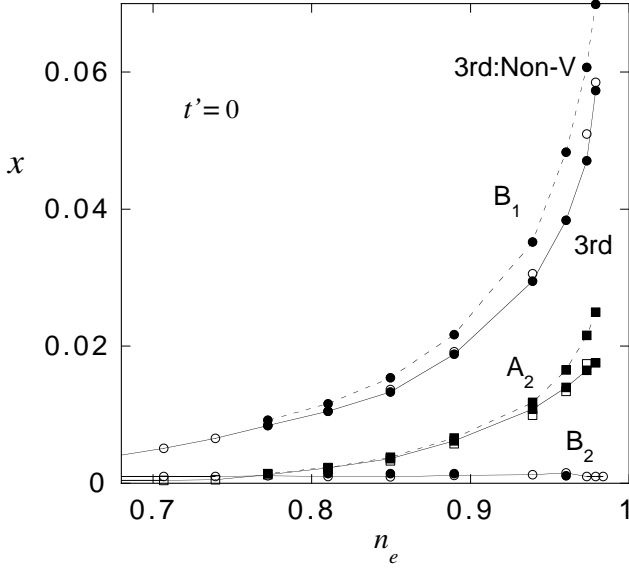


FIG. 16: The exponent  $x$  for the second-order (open symbols) and third-order (solid symbols) perturbation in  $U$ . We set  $U/t = 0.1$ . The symbol Non-V indicates the results obtained without vertex corrections.

This work was supported by Grants-in-Aid for Scientific Research from the Ministry of Education, Culture, Sports, Science and Technology of Japan. A part of numerical calculations was performed at the facilities of the Supercomputer Center of Institute for Solid State Physics, University of Tokyo.

The author expresses his sincere thanks to J. Kondo, K. Yamaji and S. Koikeyami for fruitful discussions.

## APPENDIX A: HIGHER-ORDER CORRECTIONS

In the Appendix we examine higher-order corrections to  $x$ . If the third-order terms have an effect to reduce the exponent  $x$ , the results obtained using the second-order perturbation have a possibility to become unstable as  $U$  increases. It is not an easy task to derive an effective Hamiltonian up to the third order of the interaction using the canonical transformation. The gap equation up to the third order of  $U$  has been obtained using the perturbative expansion for the Hubbard model[41, 42]. The Green's functions satisfy the Dyson equations:

$$G(\mathbf{k}, i\epsilon_n) = G_0(\mathbf{k}, i\epsilon_n) + G_0(\mathbf{k}, i\epsilon_n)\Sigma_n(\mathbf{k}, i\epsilon_n)G(\mathbf{k}, i\epsilon_n) + G_0(\mathbf{k}, i\epsilon_n)\Sigma_a(\mathbf{k}, i\epsilon_n)F^*(\mathbf{k}, i\epsilon_n), \quad (\text{A1})$$

$$F(\mathbf{k}, i\epsilon_n) = G_0(\mathbf{k}, i\epsilon_n)\Sigma_n(\mathbf{k}, i\epsilon_n)F(\mathbf{k}, i\epsilon_n) - G_0(\mathbf{k}, i\epsilon_n)\Sigma_a(\mathbf{k}, i\epsilon_n)G(-\mathbf{k}, -i\epsilon_n), \quad (\text{A2})$$

where  $\epsilon_n = (2n + 1)\pi k_B T$  is the Matsubara frequency, and  $\Sigma_n$  ( $\Sigma_a$ ) is the normal (anomalous) self-energy.  $G_0$  is the free-electron Green's function:  $G_0(\mathbf{k}, i\epsilon_n) = (i\epsilon_n -$

$\xi_k)^{-1}$ . Since we are interested in the third-order contributions,  $\Sigma_n$  (of the order of  $U^2$ ) is neglected as follows:

$$G(\mathbf{k}, i\epsilon_n) = -\frac{i\epsilon_n + \xi_k}{\epsilon_n^2 + \xi_k^2 + |\Sigma_a(\mathbf{k}, i\epsilon_n)|^2}, \quad (\text{A3})$$

$$F(\mathbf{k}, i\epsilon_n) = -\frac{\Sigma_a(\mathbf{k}, i\epsilon_n)}{\epsilon_n^2 + \xi_k^2 + |\Sigma_a(\mathbf{k}, i\epsilon_n)|^2}. \quad (\text{A4})$$

The equation for the anomalous self-energy is

$$\begin{aligned} \Sigma_a(\mathbf{k}, i\epsilon_n) = & \frac{1}{\beta N} \sum_{k', \epsilon_{n'}} [U + U^2 \chi_0(\mathbf{k} + \mathbf{k}', i\epsilon_n + i\epsilon_{n'}) \\ & + 2U^3 \chi_0(\mathbf{k} + \mathbf{k}', i\epsilon_n + i\epsilon_{n'})^2] F(\mathbf{k}', i\epsilon_{n'}) \\ & + U^3 \frac{1}{\beta^2 N^2} \sum_{k', \epsilon_{n'}, \mathbf{p}, \epsilon_\ell} G_0(\mathbf{k}', i\epsilon_{n'}) [\chi_0(\mathbf{k} + \mathbf{k}', i\epsilon_n + i\epsilon_{n'}) \\ & - \phi_0(\mathbf{k} + \mathbf{k}', i\epsilon_n + i\epsilon_{n'})] G_0(\mathbf{k} + \mathbf{k}' + \mathbf{p}, i\epsilon_n + i\epsilon_{n'} + i\epsilon_\ell) \\ & \times F(\mathbf{p}, i\epsilon_\ell) \\ & + U^3 \frac{1}{\beta^2 N^2} \sum_{k', \epsilon_{n'}, \mathbf{p}, \epsilon_\ell} G_0(\mathbf{k}', i\epsilon_{n'}) [\chi_0(-\mathbf{k} + \mathbf{k}', -i\epsilon_n + i\epsilon_{n'}) \\ & - \phi_0(-\mathbf{k} + \mathbf{k}', -i\epsilon_n + i\epsilon_{n'})] \\ & \times G_0(-\mathbf{k} + \mathbf{k}' - \mathbf{p}, -i\epsilon_n + i\epsilon_{n'} - i\epsilon_\ell) F(\mathbf{p}, i\epsilon_\ell), \quad (\text{A5}) \end{aligned}$$

for  $\beta = 1/k_B T$ . The second and third terms originate from the vertex corrections.  $\chi_0(\mathbf{q}, i\omega_m)$  and  $\phi_0(\mathbf{q}, i\omega_m)$  are defined as

$$\chi_0(\mathbf{q}, i\omega_m) = -\frac{1}{N} \sum_k \frac{f(\xi_k) - f(\xi_{k+q})}{i\omega_m + \xi_k - \xi_{k+q}}, \quad (\text{A6})$$

$$\phi_0(\mathbf{q}, i\omega_m) = -\frac{1}{N} \sum_k \frac{f(\xi_k) - f(-\xi_{-k+q})}{i\omega_m - \xi_k - \xi_{-k+q}}, \quad (\text{A7})$$

where  $\omega_m = 2\pi m k_B T$ . We assume that  $\Sigma_a$  is small and that we can neglect the  $\epsilon$ -dependence since we consider the small- $U$  limit. We set  $\Delta_{\mathbf{k}} = \Sigma_a(\mathbf{k}, \epsilon_n = 0)$ , then the equation for  $\Delta_{\mathbf{k}}$  is derived. We show the results in Fig.A for  $U/t = 0.1$  on the square lattice. The exponent  $x$  slightly decreases due to the third-order corrections. There is a cancellation among the third order terms. As has been shown in the literature[41], the vertex corrections reduce the exponent  $x$  and  $T_c$  compared to that without vertex corrections.

- 
- [1] E. Dagotto, Rev. Mod. Phys. 66, 763 (1994).
- [2] D. J. Scalapino, in *High Temperature Superconductivity - the Los Alamos Symposium - 1989 Proceedings*, edited by K. S. Bedell, D. Coffey, D. E. Deltzer, D. Pines, J. R. Schrieffer, (Addison-Wesley Publ. Comp., Redwood City, 1990) p.314.
- [3] P. W. Anderson, *The Theory of Superconductivity in the High- $T_c$  Cuprates* (Princeton University Press, Princeton, 1997).
- [4] G. R. Stewart, Rev. Mod. Phys. 56, 755 (1984).
- [5] P. A. Lee, T. M. Rice, J. W. Serene, L. J. Sham and J. W. Wilkins, Comments Cond. Matter Phys. 12, 99 (1986).
- [6] H. R. Ott, Prog. Low Temp. Phys. 11, 215 (1987).
- [7] M. B. Maple, *Handbook on the Physics and Chemistry of Rare Earths* Vol. 30 (North-Holland, Elsevier, Amsterdam, 2000).
- [8] E. Y. Loh, J. E. Gubernatis, R. T. Scalettar, S. R. White, D. J. Scalapino, and R. L. Sugar, Phys. Rev. B41, 9301 (1990).
- [9] A. Moreo, D. J. Scalapino, and E. Dagotto, Phys. Rev. B56, 11442 (1991).
- [10] J. Wheatley, Solid State Commun. 88, 593 (1993).
- [11] T. Nakanishi, K. Yamaji and T. Yanagisawa, J. Phys. Soc. Jpn. 66, 294 (1997).
- [12] K. Yamaji, T. Yanagisawa, T. Nakanishi and S. Koike, Physica C 304, 225 (1998).
- [13] A. Neumayr and W. Metzner, Phys. Rev. B67, 035112 (2003).
- [14] T. Yanagisawa, S. Koike and K. Yamaji, Phys. Rev. B 64, 184509 (2001); *ibid* B67, 132408 (2003).
- [15] T. Yanagisawa, S. Koike and K. Yamaji, J. Phys.: Condens. Matter 14, 21 (2002).
- [16] M. Miyazaki, K. Yamaji and T. Yanagisawa, J. Phys. Soc. Jpn. 73, 1643 (2004).
- [17] K. Miyake, S. Schmidt-Rink and C. M. Varma, Phys. Rev. B34, 6554 (1986).
- [18] D. J. Scalapino, E. Loh and J. E. Hirsch, Phys. Rev. B34, 8190 (1986).
- [19] J. Kondo, J. Phys. Soc. Jpn. 70, 808 (2001).
- [20] R. Hlubina, Phys. Rev. B59, 9600 (1999).
- [21] T. Schauerer and P. G. J. van Dongen, Phys. Rev. B65, 081105 (2002).
- [22] J. Kondo, private communication.
- [23] D. J. Singh and W. E. Pickett, Physica C203, 193 (1992).
- [24] D. J. Singh, Physica C212, 228 (1993).
- [25] T. Tohyama and S. Maekawa, Supercond. Sci. Technol. 13, 17 (2000).
- [26] J. M. Harris, Z. X. Shen, P. J. White, D. S. Marshall, and M. C. Schabel, Phys. Rev. B54, R15665 (1996).
- [27] K. McElory, R. W. Simmonds, J. E. Hoffman, D.-H. Lee, J. Orenstein, H. Eisaki, S. Uchida and J. C. Davis, Nature 422, 592 (2003).
- [28] D. L. Feng, N. P. Armitage, D. H. Lu, A. Damascelli, J. P. Hu, P. Bogdanov, A. Lanzara, F. Ronning, K. M. Shen, H. Eisaki, C. Kim, and Z.-X. Shen, Phys. Rev. Lett. 86, 5550 (2001).
- [29] N. E. Hussey, M. Abdel-Jawad, A. Carrington, A. P. Mackenzie and L. Ballcas, Nature 425, 814 (2003).
- [30] K. Yamaji, private communication. We thank K. Yamaji for stimulating discussions on this point.
- [31] Y. Maeno, H. Hashimoto, K. Yoshida, S. Nishizaki, T. Fujita, J. G. Bednorz, and F. Lichtenberg, Nature 372, 532 (1994).
- [32] S. Koikegami, Y. Yoshida, and T. Yanagisawa, Phys. Rev. B67, 134517 (2003).
- [33] R. H. McKenzie, Science 278, 820 (1997).
- [34] R. H. McKenzie, Comments Condens. Matter Phys. 18, 309 (1998).
- [35] K. Miyazaki, K. Kanoda, A. Kasamoto, Chem. Phys. 104, 5635 (2004).
- [36] H. Kondo and T. Moriya, J. Phys. Soc. Jpn. 73, 812 (2004).
- [37] S. Koikegami and T. Yanagisawa, J. Phys. Soc. Jpn. 70, 3499 (2001); *ibid* 71, 671 (2002).
- [38] T. Yanagisawa, S. Koikegami, H. Shibata, S. Kimura, S. Kashiwaya, A. Sawa, N. Matsubara and K. Takita, J. Phys. Soc. Jpn. 70, 2833 (2001).
- [39] T. Sato, T. Kamiyama, T. Takahashi, K. Kurahashi, and K. Yamada, 291, 1517 (2001).
- [40] C.-T. Chen, P. Seneor, N.-C. Yeh, R. P. Vasquez, L. D. Bell, C. U. Jung, J. Y. Kim, M.-S. Park, H.-J. Kim, and S.-I. Lee, Phys. Rev. Lett. 88, 227002 (2002).
- [41] T. Jujo, S. Koikegami and K. Yamada, J. Phys. Soc. Jpn. 68, 1331 (1999).
- [42] T. Nomura and K. Yamada, J. Phys. Soc. Jpn. 70, 2694 (2001).